Apr 5th, 8:00 AM

A Model Reference Adaptive Re-Entry Flight Control System

Andrew P. Sage
Professor of Electrical Engineering, University of Florida, Gainesville

A MODEL REFERENCE ADAPTIVE RE-ENTRY FLIGHT CONTROL SYSTEM

Andrew P. Sage
Professor of Electrical Engineering
University of Florida
Gainesville, Florida

SUMMARY

The pitch plane equations of motion of a rigid body maneuvering ballistic re-entry vehicle are reviewed. A quasi-linear analysis of these equations is made about a nominal re-entry trajectory. It is demonstrated that in a large number of cases constant gain compensation for the flight control system will not be satisfactory due primarily to variations in dynamic pressure and static margin. A brief review of the adaptive concept is presented. It is shown that a model reference adaptive feedback system which has lift acceleration as the controlled variable and pitch rate as a stabilizing feedback is capable of handling the re-entry control problem. Current research involving fast identification techniques is described.

RE-ENTRY DYNAMICS

In any discussion of re-entry flight control, it is necessary to deal with equations of motion of the re-entry vehicle. Solution of these equations yields range and velocity state variables as a function of initial entry states and vehicle coefficient matrix. The guidance and control system for a re-entry vehicle is designed such that a correct trade-off is achieved between range and velocity state variables and physical constraints; such as, maximum acceleration, heating rate, and heat absorbtion.

For the purposes of this paper, it will be sufficient to employ a three-degree of freedom model (longitudinal dynamics) in which velocity and altitude and hence dynamic pressure are allowed to vary. This model, commonly called a pitch plane model is a special case of the much more complicated six-degree of freedom model which in general can be analyzed only with the aid of a computer. The peripheral velocity of the earth is assumed to be negligible compared to the velocity of the re-entry vehicle. Variation of altitude during the re-entry flight is assumed negligible compared to the radius of the earth. Thus, gravitational acceleration is assumed constant. Figure 1 gives the geometry of the pitch plane model and Table 1 defines the symbols used.

Newton's second law for the motion of the center of mass of a rigid body of constant mass gives

$$\vec{F} = m \frac{d\vec{v}}{dt} \tag{1}$$

using the $\vec{i}$, $\vec{j}$ axes in Figure 1, equation 1 becomes

$$m \frac{d\vec{v}}{dt} = m \frac{dv}{dt} \vec{i} + m V \frac{d\vec{i}}{dt} = -(D + W \sin \gamma) \vec{i} + (L - W \cos \gamma) \vec{j} \tag{2}$$

But

$$\frac{d\vec{i}}{dt} = \left(\frac{d\gamma}{dt} - \frac{d\beta}{dt} \right) \vec{j} \tag{3}$$

Separating the $\vec{i}$ and $\vec{j}$ components of equations 2 and 3 and using the range angle rate equation

$$\frac{d\beta}{dt} = \frac{V}{h + r_e} \cos \gamma \tag{4}$$

and the near earth circular satellite velocity equation

$$V_s^2 = g(h + r_e) \tag{5}$$

gives

$$\sum \text{Drag Forces} \quad \frac{dV}{dt} = \frac{-D}{m} - g \sin \gamma \tag{6}$$

$$\sum \text{Lift Forces} \quad V \frac{d\gamma}{dt} = \frac{L}{m} - g \left[1 - \left(\frac{V}{V_s} \right)^2 \right] \cos \gamma \tag{7}$$

In addition, we can write the pitching moment equation

$$\sum \text{Pitch Moments} \quad \frac{d^2\theta}{dt^2} - \frac{d^2\beta}{dt^2} = \frac{P}{I_y} + \frac{T}{I_y} + \frac{M_x}{I_y} \frac{d^2\delta}{dt^2} \tag{8}$$

Other equations describing the re-entry vehicle model are

$$\text{Altitude Rate} \quad \frac{dh}{dt} = V \sin \gamma \tag{9}$$

Lift Force $$L = \frac{\rho V^2}{2} AC_L(\alpha, \delta)$$ -10-

Drag Force $$D = \frac{\rho V^2}{2} AC_D(\alpha, \delta)$$ -11-

Pitch Torque $$P = \frac{\rho V^2}{2} AC\, C_M(\alpha, \delta)$$ -12-

Range $$R = B^{r}e$$ -13-

Density $$\rho = \rho_o e^{-\beta_A h}$$ -14-

Angle of Attack $$\alpha = \theta - \gamma$$ -15-

To describe the control forces, we have reaction jet control

$$T = T_j(\alpha, \dot{\alpha}, \theta, \dot{\theta})$$ -16-

and flap control $$\delta = \delta_f(\alpha, \dot{\alpha}, \theta, \dot{\theta}, h, \dot{h}, V, \dot{V})$$ -17-

C_L and C_D are characteristic of a given vehicle. Equations of Newtonian hypersonic flow can be used to obtain a relationship between C_L and C_D as well as L/D and α. The maximum lift to drag ratio (L/D) maximum is an important design parameter since it is a measure of the maximum range of a re-entry vehicle.[1] The Newtonian formulae for a lifting body configuration (without flaps) are[2]

$$C_D = C_{D_o} + C_{D_L}\left|\sin^3\alpha\right|$$ -18-

$$C_L = C_{L_o} \cos\alpha \sin\alpha\left|\sin\alpha\right|$$ -19-

Quite often polynomial approximations to the hypersonic flow equations are used. These are, of course, quite valid for reasonably small angles of attack. Two commonly used approximations are

$$C_D \approx C'_{D_o} + C'_{D_L}\alpha^2$$ -20-

$$C_L \approx C'_{L_o}\alpha$$ -21-

Figure 2 shows typical variations of C_L, C_D, and L/D with angle of attack.

The pitching moment equation is predominantly a function of the vehicle characteristics. For small angles of attack and flap deflection, the pitching moment is normally linear as a function of angle of attack and flap deflection.

Considerable insight into the re-entry control problem can be obtained by studying the case of zero lift or ballistic entry. In almost all cases, it is reasonable to neglect the gravitational acceleration compared to the other acceleration terms present. In this case it is apparent from equation 7 that

$$\frac{d\gamma}{dt} = 0$$ -22-

or $$\gamma = \text{constant} = \gamma_E$$

thus, in the absence of gravity the re-entry vehicle will enter with a constant flight path angle. Equation 6 yields

$$G = \frac{1}{g}\frac{dV}{dt} = \frac{-D}{mg} = -\frac{1}{2}\frac{\rho V^2}{\frac{W}{C_D A}} \qquad -23-$$

Where G is the acceleration expressed in terms of g. G is also directly proportional to the dynamic pressure

$$q = \frac{1}{2}\rho V^2 \qquad -24-$$

By combining equations 23, 9, and 14 we obtain

$$\frac{dV}{d\rho} = \frac{q}{2\beta_A}\frac{V}{\frac{W}{C_D A}\sin\gamma_E} \qquad -25-$$

which yields when integrated from entry where ρ is essentially zero and V is equal to V_E up to some velocity V

$$V = V_E e^{\frac{\rho g}{2\beta_A\left(\frac{W}{C_D A}\right)\sin\gamma_E}} \qquad -26-$$

The expression for maximum acceleration can be found by maximizing G in equation 23. The result of this yields the velocity at maximum acceleration

$$V_m = V_E e^{-1/2} \qquad -27-$$

the atmospheric pressure at maximum acceleration

$$\rho m = \frac{\beta_A}{g}\left(\frac{W}{C_D A}\right)\sin\gamma_E \quad , \qquad -28-$$

and the maximum acceleration

$$G_m = \frac{\beta_A V_E^2 \sin\gamma_E}{2ge} \qquad -29-$$

which occur at the altitude for maximum acceleration

$$h = \frac{1}{\beta_A}\ln\frac{\rho g}{\beta_A \sin\gamma_E\left(\frac{W}{C_D A}\right)} \qquad -30-$$

A typical ballistic re-entry trajectory is shown in Figure 3. Figure 4 shows typical maximum acceleration (and dynamic pressure) as a function of entry angle for a ballistic entry and for a trajectory with a constant L/D = 2.

RE-ENTRY FLIGHT PATH CONTROL

The basic functions of the re-entry flight path control system are the same as those for the launch vehicle flight control system during boost. However, the severe elastic bending problems which occur during boost are normally not present or are certainly less severe in re-entry. The static margin and degree of stability will undergo rapid variations during re-entry due to the huge variation in dynamic pressure and possible thermal deformation of the re-entry body. The function of the re-entry flight path control system is to accept guidance and steering commands, perform them satisfactorily and maintain an acceptable degree of atti-

tude stability. The flight control system must be designed such that system parmeters may be adjusted as required and with sufficient speed to provide acceptable performance without requiring a priori vehicle characteristic knowledge of greater accuracy than can normally be obtained. In many cases, this will require an adaptive control system for rigid body control during the re-entry phase of flight.

A first step in the design of the flight control system is the selection of controlled variables. Generally this selection is determined by 1.) the nature of the physical constraints on the system during re-entry; 2.) the guidance and control interface; i.e., the controlled variable should be capable of reasonably simple generation by the guidance system; 3.) the ease of measuring or computing the control state variable. On this basis, the two most logical choices for controlled variables would appear to be angle of attack and lift acceleration. For the purposes of this paper, lift acceleration will be used as the control variable. Either body referenced, or inertially referenced acceleration, may be sensed in order to obtain lift acceleration.

Since the magnitude of sensible acceleration is low during the initial phase of entry, it cannot be used entirely as the controlled variable. A reaction jet system, similar to that used for on orbit control, will be used to control the vehicle during initial entry. Command signal limiting may be used to limit maximum acceleration. Since heating is proportional to the angle of attack, this will provide some measure of heating control as well.

In the design of the flight control system it is convenient to assume a flat earth with gravity negligible compared to the aerodynamic forces. Aerodynamic coefficients are assumed to be independent of Mach number, and the drag coefficient is assumed to be independent of flap deflection. In addition, a pitch reaction jet system is assumed as a source of control moment. The lift and pitching moment coefficients are linearized, and the drag coefficient is made parabolic. The approximations used are

$$C_L(\alpha, \delta) = C_{L_\alpha}\alpha + C_{L_\delta}\delta \qquad -31-$$

$$C_M(\alpha, \delta) = C_{M_\alpha}\alpha + C_{M_\delta}\delta \qquad -32-$$

$$C_D(\alpha) = C_{D_o} + C_{D_\alpha}\alpha^2 \qquad -33-$$

where α and δ are in radians.

For constant dynamic pressure and velocity, Equations 7, 8, and 15 are linear and describe the rotational behavior of the vehicle in the pitch plane.

$$V\frac{d\gamma}{dt} = q\frac{A}{m}\left[C_{L\alpha}\alpha + C_{L\delta}\delta\right] \qquad -34-$$

$$\frac{d^2\theta}{dt^2} = \frac{qAC}{I_y}\left[C_{m\alpha}\alpha + C_{m\delta}\delta\right] + \frac{T\ell}{I_y} + \frac{Mx}{I_y}\frac{d^2\delta}{dt^2} \qquad -35-$$

$$\gamma = \theta - \alpha \qquad -36-$$

These equations can be represented in block diagram form as shown in Figure 5.

$$\dot{\theta} = \frac{\left(s + \frac{qAC_{L\alpha}}{mV}\right)\left[\left(\frac{Mx}{Iy}s^2 + \frac{qAC}{Iy}C_{m\delta}\right)\delta + \frac{\ell}{Iy}T\right] - \frac{q^2A^2C_{L\delta}C_{m\alpha}}{mVIy}\delta}{s^2 + \frac{q}{m}^{A}C_{1\alpha}s - \frac{qAc}{Iy}C_{m\alpha}} \quad -37-$$

$$\alpha = \frac{\frac{\ell}{I_y}T + \left(\frac{Mx}{Iy}s^2 - \frac{qA}{MV}C_{L\delta}s + \frac{qAc}{Iy}C_{m\delta}\right)\delta}{s^2 + \frac{qA}{m}C_{L\delta}s - \frac{qAc}{Iy}C_{m\alpha}} \quad -38-$$

$$\alpha_L = \frac{\frac{qAC_{L\alpha}}{m}\frac{\ell}{Iy}T + \frac{qA}{m}\left[\left(\frac{C_{L\alpha}Mx}{Iy} + C_{L\delta}\right)s^2 + \frac{qAc}{Iy}\left(C_{L\alpha}C_{m\delta} - C_{L\delta}C_{m\alpha}\right)\right]\delta}{s^2 + \frac{qA}{m}C_{L\alpha}s - \frac{qAc}{Iy}C_{m\alpha}} \quad -39-$$

In many cases, the $C_{L\delta}$ and M_x (tail wags dog) term can be neglected. This simplifies the previous results considerably. The linearized re-entry equations can then be represented in block diagram form as shown in Figure 6. Pertinent transmission functions are now

$$\dot{\theta} = \frac{(s + qA\,C_{L\alpha}/mV)\,[(qAc/I_y)\,C_{m\delta}\delta + (\ell/I_y)]T}{s^2 + (qA\,C_{L\alpha}/mV)\,s - qAcC_{m\alpha}/Iy}, \quad -40-$$

$$\alpha = \frac{(qAc\,C_{m\delta}/I_y)\,\delta + (\ell/I_y)\,T}{s^2 + (qA\,C_{L\alpha}/mV)\,s - qAcC_{m\alpha}/Iy} \quad -41-$$

$$A_L = \frac{qA}{m}C_{1\alpha} \qquad (C_{1\delta} = Mx = 0) \quad -42-$$

If $C_{m\alpha}$ is positive, the system is unstable. It is relatively easy to show that the re-entry autopilot has unacceptably low damping for both the high q and low q cases if $C_{m\alpha}$ is negative. Stability can be provided by pitch rate feedback alone if $C_{m\alpha}$ is negative.

For the low q case, the reaction jet provides the control moment to increase damping since pitch flaps are ineffective. Normally thrust can be made directly proportional to pitch rate in order to achieve reasonable damping at low q under nominal conditions.

For high q flight, the moment obtained from the reaction jet system is inadequate and the pitch flap must be used to obtain satisfactory stability. Since large values of vehicle natural frequency are encountered at high dynamic pressures, the dynamics of the flap actuator must be considered. The control surface hydraulic system will typically have the block diagram shown in Figure 7. (7) The transfer function of the servo valve is to a very close approximation.

$$\frac{\delta a}{\delta \epsilon} = \frac{K_2}{\frac{s^2}{\omega_r^2} + \frac{2\zeta_{rs}}{\omega_r} + 1} \quad -43-$$

The transfer function of the actuator and backup structure can be assumed to be

$$\frac{\delta}{\delta a} = \frac{K_2}{s\left[\frac{s^2}{\omega_a^2} + \frac{2\zeta_{as}}{\omega_a} + 1\right]}$$

-44-

Typical numerical values for the parameters depend upon vehicle size. A not untypical set of parameter values might be

$K_1K_2 = 100$ $\quad \zeta_v = .5$ $\quad \zeta_A = .05$

$\omega_r = 500$ $\quad \omega_A = 650$

which gives a closed loop hydraulic system transfer function

$$\frac{\delta}{\delta^*} = \frac{1}{\left(\frac{s}{\omega_3} + 1\right)\left(\frac{s^2}{\omega_4^2} + \frac{2\zeta_4 s}{\omega_4} + 1\right)\left(\frac{s^2}{\omega_5^2} + \frac{2\zeta_5 s}{\omega_5} + 1\right)} \qquad 45$$

where $\omega_3 = 119$ $\quad \zeta_4 = .326$ $\quad \zeta_5 = .106$

$\omega_4 = 480$ $\quad \omega_5 = 610$

It therefore appears possible to represent the hydraulic flap actuation system as a simple lag. This must be done with great caution, however, because of the other four poles - two with very low damping. A constant gain in the pitch rate-flap control loop can be adjusted by conventional root locus, Bode diagram, or Nichol's chart techniques to achieve satisfactory response at one point - possibly maximum dynamic pressure.

In order to have zero steady state lift acceleration error for a constant lift acceleration command, it is necessary to incorporate an integration in the transfer function between lift acceleration and error to a lift acceleration command. The simplest type of fixed compensation which will give satisfactory stability augmentation appears to be proportional plus integral compensation. The resultant linearized block diagram of the qualitatively compensated system is illustrated in Figure 8.

For nominal values of system parameters (negative C_{m_α}) the values of the compensation parameters K_{a_L}, τ_{a_L}, K_{θ_T}, and K_{θ_δ} can be adjusted such that the system is sufficiently stable throughout the expected flight trajectory.

Typical Bode diagrams of the (A_y/Error) transfer function are shown in Figure 9. From this figure the phase margin for various flight conditions can be computed. It would thus appear that constant gain compensation has satisfactorily solved the flight control system design problem as long as conditions remain at the nominal values.

Closed loop acceleration response is a function of velocity V, dynamic pressure q, and the stability derivative C_{m_α}. The effects of C_{L_δ}, M_x, and the more complicated hydraulic system will have to be incorporated into the design to determine whether these terms affect the selected values of compensation parameters. Also, uncertainties in vehicle parameters, particularly the stability derivative C_{m_α}, will have to be investigated in order to determine whether the constant gain autopilot is really satisfactory. The selected values of compensation parameters will have to be altered due to the effects of C_{L_δ}, M_x, and the low damped poles in the

hydraulic system. The addition of these terms plus uncertainties in vehicle characteristics may well make it impossible to design a constant gain autopilot.

Table 2 shows some of the results of a digital computer study of conventional compensation of a high L/D re-entry vehicle. The table shows the closed loop pole zero locations for three cases of re-entry along a ballistic trajectory.

1. First order hydraulics, $M_x = C_{L\delta} = 0$, 1.5% stable static margin.
2. First order hydraulics, $M_x = C_{L\delta} = 0$, 1.5% unstable static margin.
3. Fifth order hydraulics, representative M_x and $C_{L\delta}$, 1.5% stable static margin.

In cases 1 and 2, the values of K_{aL} and τ_{aL} are constant and were adjusted such as to obtain what appeared to be the "most reasonable" response possible. For case 3 the values of K_{aL} and τ were adjusted to provide a reasonable response for that case. This required a 25% reduction in τ_{aL} and a 40% reduction in the pitch rate gain. Inspection of this table shows that non-adaptive compensation of the re-entry flight control system will be extremely difficult, if not impossible. Whether this statement will be true in general will of course depend upon many factors not considered here. Among these factors are the particular vehicle parameters used and the type of nominal trajectory (or predictively controlled trajectory) flown by the re-entry vehicle.

In order to demonstrate feasibility of a constant gain autopilot, a graph, generally multidimensional, of acceptable phase margin versus one or more of the compensation parameters and a trajectory parameter such as range and considering "worst case" values of all vehicle parameters can be calculated. This will normally appear as illustrated in Figures 10 and 11. In Figure 10 it is clear that a constant value of the parameter K can be used throughout the flight. A direct simulation would, or course, be used to verify this assertion. In Figure 11, however, there is no value of constant gain K that will give satisfactory performance throughout the entire trajectory and some form of pre-programmed adaptive or closed loop adaptive compensation must be used. The reference models and identification technique for the adaptive system will make use of the models of the re-entry flight control system discussed in this section.

ADAPTIVE CONTROL SYSTEMS

A wide variety of adaptive control systems have been proposed and studied in recent times. It appears that most of these can be included within the following three categories [8]. 1.) High gain adaptive systems. 2.) Model Reference Adaptive systems. 3.) Optimum Adaptive Systems. It should be noted that these three categories are not mutually exclusive and that a given system may be described as belonging to one or more categories depending upon the particular technique used to explain the basic adaptation operations. Various subcategories of each of the above are also possible.

The purpose of this section will be to present a brief summary of each of the above categories of adaptive systems. Particular emphasis will be placed on the model reference concepts and fast identification techniques which appear to be necessary for the re-entry flight control problem and which are under investigation currently at the University of Florida.

HIGH GAIN ADAPTIVE SYSTEMS

One of the most successful types of adaptive control systems in current use today is the high gain system such as the type provided by the Minneapolis-Honeywell Company [9] and the General Electric Company [10] for the rocket powered X-15 aircraft and other more recent applications. The high gain schemes were first proposed to meet the following requirements: (1) Zero steady state error for normal command inputs. (2) Application to a wide range of vehicles without excessive redesign and flight testing. (3) Adaptation through the variation of a single parameter. (4) Adaptation without the use of external test signals, explicit identification or limit cycling.

A schematic diagram of a high gain system is shown in Figure 12. In this high gain system, the gain in the feedback loop around the nonstationary process is kept as high as possible in order that some closed loop poles of the nonstationary process approach the location of model zeros. Since these zeros are in the feedback loop, they do not appear in the closed loop transfer function even though they influence the shape of the root locus. Thus, the dominant closed loop poles are typically near the model zeros. Monitoring is provided as a check for oscillations produced by high gain associated instabilities. Thus, the system is adjusted so that its response is kept close to that of a particular model regardless of the varying process parameters. A typical root locus is shown in Figure 13 with the gain set to produce the pole zero pattern on the root locus indicated by the triangles. The model zeros do not appear in the closed loop transfer function between input and output since they are in the feedback path.

Needless to say, not all of the original expectations concerning high gain adaptive systems have materialized. Nonlinearities and noise in particular can cause serious difficulties in operation of the high gain schemes. Limit cycling has posed a problem. Considerable simulation and flight testing of the high gain schemes has been necessary due to the lack of adequate analytical design procedures. This author knows of no published work specifically applying the high gain scheme to re-entry flight control.

MODEL REFERENCE ADAPTIVE SYSTEMS

In this approach, a reference model is employed as part of the adaptive loop. The model represents "ideal" performance characteristics of the closed loop dynamic process. The difference between the model response and actual system response is an error signal which the adjusting process uses to adjust one or more system parameters in order to cause the actual system to approximate the model. Figure 14 shows a generalized model reference system. Model reference adaptive systems can be separated into one of several categories depending upon the makeup of the adaptive loop.

1. Adaptive loop input signals
   a. normal control loop signals
   b. external test signals
2. Control loop modification methods
   a. parameter adjustment methods
   b. parameter perturbation methods
   c. signal synthesis methods
3. Adjusting mechanism system model
   a. explicit model
   b. implicit (identified) model

4. Adjusting mechanism decision techniques
   a. performance index techniques
   b. gradiant techniques
   c. second method techniques

Adaptive Loop Input Signals

The operation of the adaptive loop may be with normal operating control signals or with external test signals. Generally, "faster" adaptation will occur when normal operation signals are used. Use of normal operating signals in the adaptive loop may present an adaptive loop stability problem for some signals and will generally prevent analytical design of the adaptive loop.

Control Loop Modification Methods

By far the most widely used method of control loop modification is parameter adjustment,[11, 12, 13] in which the parameters of the various compensation elements are adjusted such that the error signal is minimized. In the parameter perturbation technique[14,15] a system parameter is perturbed with a small sinusoidal fluctuation The error exhibits an oscillatory component at this same frequency. The parameter is then adjusted in such a fashion that the time average of the error function is minimized. In the control signal snythesis method,[16] control loop modification consists of generation of a signal, added to the basic dynamic system such that the "error" between the model and the dynamic system is minimized.

Adjusting Mechanism System Model

If the adjusting mechanism uses an identified model to represent the unknown physical system, the adjusting mechanism is then said to use an implicit model. If the adjusting mechanism uses some reasonable assumption as to the needed data on the dynamic performance characteristics of the system (such as provided by the reference model) the adjusting mechanism is then said to use an explicit model.

Adjusting Mechanism Decision Techniques

Three basic adjusting mechanism decision techniques have been discussed in the literature. The basis for operation of the performance index technique is the minimization of the integral of a quadratic function of the error and its derivatives. Two typical performances indices are

$$J_1 = \frac{1}{2}\int\left\{a_o\, e(t) + a_1 \frac{de}{dt} + a_2 \frac{d^2e}{dt^2} + a_3 \frac{d^3e}{dt^3}\right\}^2 dt \qquad -46-$$

$$J_2 = \frac{1}{2}\int\left\{b_o\, e^2(t) + b_1\left(\frac{de}{dt}\right)^2 + b_2\left(\frac{d^2e}{dt^2}\right)^2 + b_3\left(\frac{d^3e}{dt^3}\right)^2\right\} dt \qquad -47-$$

Some partial derivatives of the performance index must be zero in order for the performance index to be minimum. The term "error quantity" has been used by the M.I.T. group which originally investigated this type of adaptive system to indicate the need for parameter adjustment. For Equation 47 with $b_2 = b_3 = 0$ and slowly varying P_n

$$(EQ)_n = \frac{\partial}{\partial P_n} J_2 \cong \int\left\{b_o\, e(t)\frac{\partial e}{\partial P_n} + b_1 \frac{de}{dt}\frac{d}{dt}\left(\frac{\partial e}{\partial P_n}\right)\right\} dt \qquad -48-$$

The terms $\partial e/\partial P_n$ and $d/dt\ (\partial e/\partial P_n)$ are called error weighting functions $W_n(t)$ and

d W_n/dt. Since the model output is not a function of P_n, the error weighting functions become $\partial c/\partial P_n$ and $d/dt(\partial c/\partial P_n)$ which cannot be evaluated without identification of the dynamic characteristics of the system. Figure 15 illustrates the M.I.T. method of explicit generation of the error quantity for a particular case in which P_n is a forward loop gain. In terms of Laplace transforms (for slowly varying P_n)

$$W_n(s) = \frac{\partial E(s)}{\partial P_n} = \frac{\partial c(s)}{\partial P_n} = \left[\frac{G_1(s)\,G_2(s)}{1 + G_1(s)\,P_n\,G_2(s)}\right]\left[\frac{R(s)}{1 + G_1(s)\,P_n\,G_2(s)}\right] \qquad -49-$$

The first term in this expression represents the closed loop poles and zeros of the system. The last term is the Laplace transform of the signal E_1. If it is assumed that the model is an accurate representation of the system then the model transfer function may be used instead of the system function as a weighting function filter to yield Figure 15. Osburn[17] has demonstrated by appropriate simulations that this approximation works very well when an accurate model is chosen and when the unknown system parameters are near those of the model. The derivative error weighting function $d\,W_n/dt$ can be generated in a similar fashion. The adjustable parameter P_n is then adjusted in accordance with an appropriate linear differential equation.

$$\sum_{i=1}^{\ell} \alpha_i \frac{\partial^i P_n}{dt^i} = \sum_{j=1}^{m} \beta_j \frac{\partial^j (EQ)_n}{\partial t^j} \qquad -50-$$

$$P_n(s) = A(s)\,[EQ]_n\,(s) \qquad -51-$$

or possibly even a nonlinear differential equation. The basic M.I.T. system uses a rate of change of the parameter directly proportional to the slope of the error quantity

$$\frac{\partial P_n}{dt} = -\,b_o\,e(t)\,W_n(t) \qquad -52-$$

The response characteristics of the adaptive loop are of course dependent upon the adaptive loop transfer characteristics given by Equation 50, as well as the explicit or implicit model used in the adjusting system and the input signal $r(t)$. Since the adaptive loop is nonlinear, a simple stability analysis or compensation procedure is not available. The adaptive loop may be linearized by letting

$$P_n(t) = P_{n_{Nominal}} + \Delta P_n(t) \qquad -53-$$

and by dropping the products of dependent variables in writing the equations of the adaptive loop. This yields the linear time varying system of Figure 16 where it is assumed that the model is of the same order as the system with

$$P_{n_{Model}} = P_{n_{Nominal}} = P_{nN} \qquad -54-$$

If the coefficient matrix or transfer function of the model is considerably different from that of the system, the linearized model of the adaptive loop is much more complicated. In this linearized model, it is apparent that adaptive loop stability is greatly dependent on the input signal. If a "fast" adaptive loop is to be designed, it seems reasonable to expect that a standard test input $r(t)$ should be used in the adaptive loop.

In order to operate the adaptive portion of the loop with non normal test signals an identification technique can be used to establish the characteristic para-

meters of the physical system. This identified system will also serve as the implicit model for the weighting function filter. Preliminary results of an identification technique investigation using sinusoidal test signals and a time variable transform are discussed in the next section. Once the characteristics of the unknown dynamic system are identified, any r(t), convenient for adaptive loop design purposes, may be applied to the identified model in order to determine parameter adjustments for the control loop.

The basis for the gradiant decision technique consists of formulation and minimization of a quadratic function of the error, e(t) and its derivatives.[18] This minimization is achieved by forming the gradient vector of the error adjusting appropriate system parameters on an incremental basis such as via a steepest descent procedure until the minimization of the error functional is achieved. The differences between the gradient approach and the performance index approach are primarily in terms of the initial adaptive loop problem formulation. The two methods generally lead to essentially the same end result.

In the area of adjusting method decision techniques, use of the second method Liapunon has been proposed to give insight as well as a method of approach.[19] Since it is desired to alter the control loop in order to cause the unknown system to appear like the model, the error between the plant and the model must be asymptotically stable. A positive definite Liapunov function is formed for the error equation, e(t). The adjusting mechanism equations are selected so as to cause the time derivative of the Liapunov function to be as negative definite as possible. This insures asymptotic stability and "tends towards" time optimal performance of the adaptive loop.[20] As might be expected there is considerable similarity between this method and the gradient and performance index techniques.

Optimal Adaptive Control Systems

One very complex but highly promising form of adaptive control is on line optimal adaptive computer control. The basic theory of optimal control has been developed by Pontryagin, Bellman, Kalman, and others. Most of this theory assumes that (1) the components of the state vector can be measured exactly and fed back in the mechanization of the optimal system, (2) the value of the system parameters (system characteristic matrix) is known exactly. Application of optimization theory to cases where these assumptions are not valid results in optimal adaptive control.

A rather general sketch of one method for implementing optimal adaptive control is shown in Figure 17. The inputs to the optimum control computer consists of the identified model of system dynamics and the performance index. The output of the optimal control computer will be the optimal (or suboptimal) control vector $\underline{\mu}_o$, which will be used (in conjunction with any low level test input signal) as the process input.

The performance criterion will generally be specified by guidance accuracy requirements in conjunction with constraints imposed by heating and maximum acceleration requirements. Thus the performance index PI can be expressed as a function

$$PI = \int_{t_o}^{T} g(\underline{\mu}, \underline{x}, t)\, dt + h\,[\underline{x}(t), T] \qquad \text{-55-}$$

The performance index is generally simplified by dropping terms which are small in comparison to dominant terms. Since the identification of re-entry dynamics will be subject to some non-reducible error, there will be nothing gained in refining the performance criterion beyond a certain point.

The calculus of variations may be applied to determine necessary conditions for a maximum or minimum of equation 55. The calculus of variations treats continuous decision problems which are limiting cases of multistage decision problems (dynamic programming) where the time increment between steps becomes small compared to the time of interest. Actually the reverse problems are more common today. Continuous problems are approximated by multistage decision problems for solution on a digital computer.

The task of the optimal control computer is to maximize or minimize the performance index subject to the equality constraint that

$$\dot{\underline{x}} - f(\underline{x}, \underline{\mu}, t) = 0 \qquad -56-$$

which is the vector differential equation describing the re-entry and actuator dynamics.

Following the usual variational procedure, the process differential equation is adjoined to the performance index with a Lagrange multiplier vector $\underline{\lambda}(t)$ to give

$$PI = h[\underline{x}(T), T] + \int_{t_o}^{T} \{g[\underline{\mu}(t), \underline{x}(t), t] + \underline{\lambda}'(t) \left\langle f[\underline{x}(t), \underline{\mu}(t), t] - \dot{\underline{x}} \right\rangle\} dt \qquad -57-$$

A scalar function H (the Hamiltonian) is defined as

$$H[\underline{x}(t), \underline{\mu}(t), t] = g[\underline{x}(t), \underline{\mu}(t), t] + \underline{\lambda}'(t) f[\underline{x}(t), \underline{\mu}(t), t] \qquad -58-$$

The performance index upon integrating by parts becomes

$$PI = h[\underline{x}(T), T] - \underline{\lambda}'(T)\underline{x}(T) + \underline{\lambda}'(t_o)\underline{x}(t_o) + \int_{t_o}^{T} \{H[\underline{x}(t), \underline{\mu}(t), t] + \dot{\underline{\lambda}}'(t)\underline{x}(t)\} dt \qquad -59-$$

The variations in the performance index due to variations in the control vector $\underline{\mu}(t)$ and state vector $\underline{x}(t)$ (for fixed T) are

$$\Delta_{PI} = \left[\frac{\partial h}{\partial \underline{x}} - \underline{\lambda}'\right]_{t=T} \Delta\underline{x} + \left[\underline{\lambda}'(t_o)\,\Delta(\underline{x})\right]_{t=t_o} + \int_{t_o}^{T} \left\{\left(\frac{\partial H}{\partial \underline{x}} + \dot{\underline{\lambda}}'\right)\Delta\underline{x} + \frac{\partial H}{\partial \underline{\mu}}\Delta\underline{\mu}\right\} dt \qquad -60-$$

Since the variation is independent of small changes in $\underline{x}(\Delta\underline{x})$ if the performance index in a true maximum (or minimum) it follows that

$$\dot{\underline{\lambda}}' = -\frac{\partial H}{\partial \underline{x}} \qquad \text{and} \qquad \underline{\lambda}'(T) = \frac{\partial h}{\partial \underline{x}} \qquad \begin{matrix} -61a- \\ -61b- \end{matrix}$$

Equation 61a is called the adjoint equation and equation 61b gives the boundary conditions for the adjoint at the terminal time. The variation in the performance index then becomes

$$\Delta_{PI} = \underline{\lambda}'(t_o)\,\Delta\underline{x}(t_o) + \int_{t_o}^{T} \frac{\partial H}{\partial \underline{\mu}}\Delta\underline{\mu}\, dt \qquad -62-$$

For an extremum, Δ_{PI} must be zero for arbitrary $\Delta\underline{\mu}$ and this can only happen if

$$\frac{\partial H}{\partial \underline{\mu}} = 0 \qquad t_o < t < T \qquad -63-$$

This is a very simplified development of the Pontryagin Maximum Principle[21] and is not, in its present form, as general as the maximum principle of Pontryagin.

For linear systems, the principle of superposition can be invoked and solutions obtained without much difficulty. In fact, if

$$PI = \tfrac{1}{2}\,\underline{x}'(T)\,S\,\underline{x}(T) + \tfrac{1}{2}\int_{t_o}^{T} \{[C(t)\,\underline{x}(t)]'\,Q(t)\,C(t)\,\underline{x}(t) + \underline{\mu}'R(t)\underline{\mu}\}\,dt \qquad -64-$$

and if

$$\dot{\underline{x}} = A(t)\,\underline{x} + B(t)\,\underline{\mu}$$

$$\underline{y}(t) = C(t)\,\underline{x}(t)$$

the optimal control law is linear and time varying

$$\underline{\mu}(t) = K(t)\,\underline{x} \qquad -65-$$

$$K(t) = -R^{-1}(t)\,B'(t)\,P(t)\,\underline{x}(t) \qquad -66-$$

where P(t) is the solution to the matrix Riccati equation

$$-\frac{dP}{dt} = A'P + PA - PBR^{-1}B'P + C'QC \qquad -67-$$

with the terminal condition

$$P(T) = S \qquad -68-$$

For this case the optimal controller is a linear time varying feedback system in which all state variables of the system must be known at all times to effect control. This optimal control scheme was first proposed by Kalman[22] Attempts have been made by several investigators to extend and simplify this method of optimal control.[23]

In order to apply this technique to the re-entry problem it is necessary to determine a nominal trajectory and linearize the re-entry dynamics about this nominal trajectory. An example of interest is the lambda matrix control scheme which Denham and Bryson [24] have applied to the guidance of a low L/D vehicle which enters the atmosphere at supercircular velocity. Bryson and Denham propose a re-entry scheme which uses aerodynamic braking and lift for control purposes.

The essential features of the lambda matrix control consist of storage in a fixed memory for a sufficient number of nominal trajectories and associated lambda matrices. (Time varying feedback gains). These must be sufficient to cover the expected range of re-entry velocities and corridors of possible initial entry angles associated with each re-entry velocity. The control law for re-entry guidance takes the form

$$\left(\frac{L}{D}\right)_{\text{control}} = \left(\frac{L}{D}\right)_{\text{nominal}} + \Lambda_V\,\delta_V + \Lambda_h\,\delta h + \Lambda_R\,\delta R + \Lambda_\gamma\,\delta\gamma \qquad -69-$$

where Λ represents the gains (lambda matrices) determined by the Wiener Kalman optimization procedure. A block diagram of the lambda matrix guidance scheme is shown in Figure 18.

Unfortunately the optimum control law is in general strictly unrealizable for any but systems with known dynamics. The Riccati equation must be solved backward in time from t = T to t = o which requires knowledge of A(t) over the interval 0 to T. In general this information is not available at t = o. Thus it is necessary to obtain from identification of the re-entry dynamics some prediction of A(t), B(t), and C(t) into the future at least as far as several time constants of the Riccati equation for the control problem. Methods for doing this have not been developed, but are the subject of much current research. When accomplished, this will remove the restriction that the system parameters be known exactly throughout the entire re-entry.

Normally, the state vector $\underline{x}$ cannot be observed directly. What is observed is

a vector $\underline{y}$ which is corrupted by noise. Mathematically this is expressed as

$$\dot{\underline{x}} = A(t)\ \underline{x} + W(t) + B(t)\ \underline{u}(t) \qquad -70-$$

$$\underline{y}(t) = C(t)\ \underline{x}(t) \qquad -71-$$

$$\underline{z}(t) = \underline{y}(t) + \underline{v}(t) \qquad -72-$$

often $W(t)$ and $V(t)$ are uncorrelated zero mean Gaussian random vectors with covariance matrices

$$E\ \{V(t)\ V^T(\tau)\} = R_{vv}(t, \tau) = \bar{R}(t)\ \delta(t-\tau) \qquad -73-$$

$$E\ \{W(t)\ W^T(\tau)\} = R_{ww}(t, \tau) = \bar{Q}(t)\ \delta(t-\tau) \qquad -74-$$

The filtering problem of optimal adaptive control consists in determining a linear operator on the set $\underline{z}(t)$ of observations $0 < t < t$ whose value $\hat{\underline{x}}(t_1/t)$ is the unbiased minimum variance estimate of $\underline{x}(t)$. Kalman has shown that $\hat{\underline{x}}(t/t)$ is the output of a dynamic system governed by the equation

$$\frac{d\hat{\underline{x}}}{dt}(t/t) = A(t)\ \hat{\underline{x}}\ (t/t) + K(t)\ \ [\underline{z}(t) - C(t)\ \hat{\underline{x}}\ (t/t)] \qquad -75-$$

where $K(t)$, the gain of the optimal filter is determined by the covariance matrix of the errors of the optimal filter

$$K(t) = \Sigma(t)\ C'(t)\ \bar{R}^{-1}\ (t) \qquad -76-$$

where

$$\frac{d\Sigma}{dt} = A(t)\ \Sigma + \Sigma\ A'(t) - \Sigma\ C'(t)\ \bar{R}^{-1}\ (t)\ C(t)\ \Sigma + \bar{Q}(t) \qquad -77-$$

with

$$\Sigma(t_o) = E\ \{x\ (t_o)\ x'(t_o)\ \} \qquad -78-$$

The Riccati equation for the filtering problem (variance equation) is solved forward in time. Thus the solution to the filtering problem is completely realizable. Much current effort is attempting to answer unresolved questions concerning optimal adaptive control. The largest unexplored areas appear to concern proper identification techniques and selection of appropriate performance indices. It appears that optimal adaptive control will have more direct applications to guidance or integrated guidance and flight control systems than it will have to flight control system design.

FAST IDENTIFICATION FOR MODEL REFERENCE ADAPTIVE SYSTEMS

Current research is being undertaken by this author and W. Clay Choate in order to determine ultimate performance limitations for a particular fast identification technique which is proposed in order to allow the adaptive loop of a model reference parameter adjustment system to operate with external inputs and to provide an implicit model for the weighting function filter. Although the intended application is for model reference systems, the technique may be useful for identification in optimal adaptive systems as well.

The technique is based on the time varying frequency transform of Zadeh.[25] Use is made of the property that this transform satisfies a linear ordinary differential equation closely related to the differential equation which describes the dynamics of the re-entry system. Provided the transform can be measured, it can be substituted into its differential equation, and the coefficients of the equation determined. Through algebraic manipulation of these coefficients, the characteristic matrix of the differential equation describing the unknown system may be obtained. Periodic repetition of this procedure permits the time variation of the system to be discerned.

To formulate the problem in mathematical terms, the single input linear system, described by

$$p\underline{x} = A(t)\,\underline{x} + B(t)\,\underline{y} \qquad -79-$$

$$\underline{y} = C\underline{x} + D\underline{y}\,, \qquad -80-$$

is considered. In these equations

$p \triangleq d/dt$ (differential operator

$\underline{x}$ is the n-dimensional state vector

$$\underline{x}' = [x_1, x_2, \ldots x^n] = [x, Px, \ldots, P^{n-1}X] \qquad -81-$$

$\underline{y}$ is the 1-dimensional output vector defined by equation 80 in terms of the known matrices C and D.

It is assumed that at least the first component x_1 of $\underline{x}$ can be obtained instantaneously from $\underline{y}$.

$\underline{\mu}$ is the m-dimensional input vector, related to the single (scalar) input μ according to the equation

$$\underline{\mu}^T = [\mu, P\mu, \text{---}, P^{m-1}\mu] \qquad -82-$$

Matrices A(t) and B(t) are not known completely, but are assumed to have the forms

$$A(t) = [a_{ik}(t)] = \begin{bmatrix} 0 & 1 & 0 & \cdots & 0 \\ 0 & 0 & 1 & \cdots & 0 \\ \cdot & \cdot & \cdot & \cdot & \cdot \\ 0 & 0 & 0 & \cdots & 1 \\ a_{n1}(t) & a_{n2}(t) & a_{n3}(t) & \cdots & a_{nn}(t) \end{bmatrix} \qquad -83-$$

$$B(t) = [b_{ik}(t)] = \begin{bmatrix} 0 & 0 & 0 & \cdots & 0 \\ 0 & 0 & 0 & \cdots & 0 \\ \cdot & \cdot & \cdot & \cdot & \cdot \\ 0 & 0 & 0 & \cdots & 0 \\ b_{n1}(t) & b_{n2}(t) & b_{n3}(t) & \cdots & b_{nm}(t) \end{bmatrix} \qquad -84-$$

or are assumed to be convertable to these forms by a linear non-singular transformation of variable in equation 79. Thus, phrased in terms of equation 79, the identification problem becomes that of determining the time functions

$$a_{ni}(t),\ i = 1, \ldots, n \qquad -85-$$
$$b_{nk}(t),\ k = 1, \ldots, m$$

of matrices A(t) and B(t). In the general case, some of the n + m functions of equation 85 may be known a priori. This situation, of course, simplifies the identification problem, and will be discussed later.

The time varying frequency transform $\underline{h}(j\omega, t)$ is defined as

$$\underline{h}(j\omega,t) = T(j\omega)\,\underline{\chi}(j\omega,t) \qquad -86-$$

where

$$T(j\omega) = [t_{ik}(j\omega)] \qquad -87-$$

$$t_{ik}(j\omega) = \frac{i!\,(-j\omega)^{i-k}}{k!\,(i-k)!} = \begin{bmatrix} i \\ k \end{bmatrix} (-j\omega)^{i-k}, \quad i \geq k \qquad -88-$$

$$t_{ik}(j\omega) = 0, \quad i < k \qquad -89-$$

$$|T(j\omega)| = 1 \qquad -90-$$

$$\underline{\chi}(j\omega,t) = \int_{-\infty}^{\infty} \underline{W}(t,\xi)\, e^{-j\omega(t-\xi)}\, d\xi \qquad -91-$$

$\underline{W}(t,\xi)$ is the response of the state variable when the input is a unit impulse occurring at time $t = \xi$. It may be readily verified the definition gives the following property to the elements of $\underline{h}(j\omega,t)$

$$h_i(j\omega,t) = ph_{i-1}(j\omega,t), \quad i = 2, \ldots, n \qquad -92-$$

While $\underline{h}(j\omega,t)$ is defined in terms of the impulse response of equation 79, it is possible to express it in terms of the response of equation 79 to sinusoidal excitation. In fact, an alternate definition of $\underline{h}(j\omega,t)$ is

$$\underline{h}(j\omega,t) = e^{-j\omega t}\, T(j\omega)\, \underline{\xi}(j\omega,t) \qquad -93-$$

where $T(j\omega)$ is defined in equation 87 and $\underline{\xi}(j\omega,t)$ is the response of equation 79 to $u = e^{j\omega t}$. The proposed identification scheme makes use of equation 93 as a means for determining $\underline{h}(j\omega,t)$.

The elements of $\underline{h}(j\omega,t)$ belong to the field of complex numbers. Since measurements necessarily involve real numbers, it is convenient to break this vector into real and imaginary components. Using the abbreviation $\underline{h} \triangleq \underline{h}(j\omega,t)$ and the notation subscript "R" for "real part of ..." and subscript "I" for "imaginary part of ...", and regarding ω as a fixed parameter, it can be shown that

$$P \begin{bmatrix} \underline{h}_R \\ - - \\ \underline{h}_I \end{bmatrix} = \left[\begin{array}{c|c} E_R(j\omega,t) & -E_I(j\omega,t) \\ - - - - - & - - - - - \\ E_I(j\omega,t) & E_R(j\omega,t) \end{array}\right] \begin{bmatrix} \underline{h}_R \\ - - \\ \underline{h}_I \end{bmatrix} + \begin{bmatrix} \underline{k}_R(j\omega,t) \\ - - - - \\ \underline{k}_I(j\omega,t) \end{bmatrix} \qquad -94-$$

where the n X n matrix $E(j\omega,t)$ is of the general form of $A(t)$ with elements $\{e_{nr}(j\omega,t)\}$ related to the elements $\{a_{ni}(t)\}$ of $A(t)$ by the equations

$$e_{nr}(j\omega,t) \sum_{k=r}^{n+1} \frac{(k-1)!\,(j\omega)^{k-r}}{(r-1)!\,(k-r)!}\, a_{nk}(t) \quad ; \qquad -95-$$

the additional element $a_{n,n+1}(t)$ is taken to be -1. The n-vector $\underline{k}(j\omega,t)$ is related to matrix $B(t)$ of (79) by

$$\underline{k}(j\omega,t) = B(t) \begin{bmatrix} 1 \\ j\omega \\ \vdots \\ (j\omega)^{m-1} \end{bmatrix} \qquad -96-$$

If $\underline{h}$ and $p\underline{h}$ are available, substitution in equation 94 gives with the aid of equation 95 and equation 96 two algebraic equations in the functions of equation 85. Measurements of $\underline{h}$ at q frequencies $\omega_1, \omega_2, \ldots, \omega_q$, $i > k \Rightarrow \omega_i > \omega_k$, gives 2q such equations. Assuming that s of the $n^2 + m$ functions are known apriori, it follows that the matrices $A(t)$ and $B(t)$ can be identified if

$$q = \tfrac{1}{2}(n + m - s) \qquad \text{or} \qquad q = \tfrac{1}{2}(n + m + 1 - s) \qquad \text{-97-}$$

depending upon which is the integer.

Consider briefly the problem of measuring the time varying transform. For a test signal

$$\tilde{u} = \sum_{i=1}^{q} \cos \omega_i t \qquad \text{-98-}$$

applied as input, the response of the system is, by equation 93 and the principle of superposition,

$$\tilde{\underline{x}}(t) = \sum_{i=1}^{q} \{ [T^{-1}(j\omega_i)\underline{h}(j\omega_i,t)]_R \cos \omega_i t + [T^{-1}(j\omega_i)\underline{h}(j\omega_i,t)]_I \sin \omega_i t \} \qquad \text{-99-}$$

Since the non-singular matrix $T(j\omega)$ is known, $\underline{h}(j\omega_i,t)$, $i = 1, \ldots, q$, may be measured by demodulation of $\tilde{\underline{x}}(t)$.

The bifrequency transform is defined as

$$\underline{\Gamma}(j\omega_i, j\mu) = \int_{-\infty}^{\infty} \underline{h}(j\omega_i, t)\, e^{j\omega_i t}\, e^{-j\mu t}\, dt \qquad \text{-100-}$$

it can be shown that successful demodulation of equation 99 requires that

$$\| \underline{\Gamma}(j\omega_i, j\mu) \| \cong 0 \text{ for } \mu \cong 0 \quad \text{and} \quad \mu \geq \omega_1 \qquad \text{-101-}$$

and

$$\left\langle \underline{\Gamma}(j\omega_i, j\mu), \underline{\Gamma}(j\omega_{i+1}, j\mu) \right\rangle \cong 0 \; \forall \; \mu \qquad \text{-102-}$$

and $\forall\, i = 1, 2, \ldots, q-1$.

Since the bandwidths of the $\underline{\Gamma}(j\omega_i, j\mu)$ increase as the rates of parameter variations increase, rapidly changing systems require large and widely separated test frequencies. However, greater attenuation of high frequency components by the average system makes measurement of $\underline{h}(j\omega,t)$ more difficult in this case. Further, it can be shown that the operations leading from (13) to (1) become more sensitive to measurement errors when the frequency is large. For this reason, the best choice of test signal frequencies depends, in part, on the noise present. The investigation of this problem will be the subject of another paper.

The proposed identification scheme becomes difficult to implement when the order of the system is high, particularly if (2) cannot be solved for the state vector $\underline{x}$. However, if the system can be broken down into a stationary part and a low order time varying part, the identification procedure becomes much simpler. In fact, if the time varying part follows the stationary part, the identification is no more difficult than if only the time varying part were to be identified.

The following areas are now under consideration:

1. Computer simulation of "fast" identification schemes

2. Theoretical and experimental studies of problems resulting from the

presence of guidance commands in the adaptive loop.

3. Evaluation of the merits of different test signals.

4. Simulation and analytical study of closed loop implicit parameter adjusting model reference re-entry systems.

Final evaluation of this proposed method for re-entry flight path control will depend upon completion of the above tasks and will be reported in the near future.

REFERENCES

1. Wang, K., and Ting, L.: Analytic Solutions of Planar Re-Entry Trajectories With Lift and Drag. Polytechnic Institute of Brooklyn (PIBAL) Rep. No. 601 (April 1960).
2. Wang, H. E.: Hypersonic Aerodynamics and Re-Entry Heating." Lecture notes for short course "Guidance and Control of Re-Entry Vehicles." X414.11 (August 1963) UCLA.
3. Allen, H. Julian, and Eggers, A. J., Jr.: A Study of the Motion and Aerodynamic Heating of Ballistic Missiles Entering the Earth's Atmosphere at High Supersonic Speeds. NASA Rep. 1381, 1958.
4. Chapman, Dean R.: An Approximate Analytical Method for Studying Entry Into Planetary Atmospheres. NASA TR R-11, 1959.
5. Wingrove, Rodney C.: "Survey of Atmosphere Re-Entry Guidance and Control Methods," AIAA Journal, Vol. 4, Number 9, September 1963.
6. Volgenau, Ernest: "Boost Glide and Re-Entry Guidance and Control," Chapter 10 of Guidance and Control of Aerospace Vehicles, Edited by Leondes, Cornelius T., McGraw-Hill, 1964.
7. Thayer, W. J.: Transfer Functions for Moog Servovalves, Technical Bulletin No. 103, December, 1958.
8. Kishi, Francis.: "On Line Computer Control Techniques and Their Application to Re-entry Aerospace Vehicle Control," Chapter 6 of Advances in Control Systems, Volume I, Edited by C. T. Leondes Academic Press, 1964.
9. Mellon, D. L.: "Applications of Adaptive Flight Control," Proceedings of the First International Symposium on Optimizing and Adaptive Control, Instrument Society of America (1962).
10. Buscher, R. G., Haefner, K. B., and Marx, M. F.: Self Adaptive Flight Control Through Frequency Regulation, IEEE Wescon Proceedings, 1961.
11. Whitaker, H. P., Yarmon, J., and Kezer, A.:"Design of Model Reference Adaptive Control Systems for Aircraft," MIT Instrumentation Laboratory Report R-164, September 1958.
12. Whitaker, H. P.: "Model Reference Adaptive Control Systems for Large Flexible Boosters," MIT Instrumentation Laboratory Report E-1036, May 1960, Presented to SAE-18 Committee on Aerospace Vehicle Flight Control Systems on 16 June 1961.
13. Margolis, M., and Leondes, C. T.: "A Parameter Tracking Servo for Adaptive Control Systems," IRE Transactions on Automatic Control, PGAC 4, No. 2:100-111, November 1959.
14. McGrath, R. J., Rideout, V. C.: "A Simulator Study of a Two Parameter Adaptive System," IRE Transactions on Automatic Control, Vol. AC-6, No. 1, February 1961.
15. McGrath, R. J., Rajaraman, V., and Rideout, V. C.: "A Parameter Perturbation Adaptive Control System," IRE Transactions on Automatic Control, Vol AC-6, No. 2, May 1961.

16. Hiza, J. G. and Li, C. C.: "On Analytical Synthesis of a Class of Model-Reference Time-Varying Control Systems," IEEE Paper 63-123, IEEE Transactions on Applications and Industry, November 1963.
17. Osburn, P. V.: "Investigation of a Method of Adaptive Control," Doctor of Science Thesis, Massachusetts Institute of Technology, 1961, MIT Instrumentation Laboratory Report No. T 266.
18. Donalson, D. D.: "The Theory and Stability Analysis of a Model Referenced Parameter Tracking Technique for Adaptive Automatic Control Systems," Doctorate Dissertation, University of California, Los Angeles, May 1961.
19. Rang, E. R., and Stone, C. R.: "Adaptive State Vector Control, Adaptive Controllers Derived by Stability Considerations," Minneapolis-Honeywell Regulator Company, Military Products Group Report 1529-TR 9, 15 March 1962.
20. Melsa, J. L.:"Closed Loop Suboptimal Control Using the Second Method of Liapunov," University of Arizona, Ph.D. Thesis, December 1964.
21. Pontryagin, L. S., Boltyansky, R. V., Gamkrelidze, R. V., and Mishchenko, Y. F.: "Mathematical Theory of Optimal Processes," Interscience Division of John Wiley & Sons, 1963.
22. Kalman, R. E.:"Fundamental Study of Adaptive Control Systems," Technical Report ASD-TDR 61-27 (April 1962).
23. Sage, A. P., and R. B. Streets: "Synthesis of Approximately Optimal Control Systems Using Bode Diagrams," Proceedings 1964 Allerton Conference on Circuit and System Theory.
24. Bryson, A. E., and Denham, W. F.: "A Guidance Scheme for Supercircular Re-Entry of a Lifting Vehicle," Paper presented at ARS Space Flight Report to the Nation, October 1961. ARS J32, 894-898 (1962).
25. Zadeh, L. A.: "Frequency Analysis of Variable Networks," Proceedings IRE Vol. 38, pp 201-299, 1950.

TABLE I - LIST OF SYMBOLS

A_L	Lift acceleration
A	Airframe characteristic area, usually taken to be the wing planform area
c	Airframe characteristic length, usually taken to be the wing base chord
C_D	Dimensionless coefficient of drag
C_L	Dimensionless coefficient of lift
C_M	Dimensionless coefficient of pitching moment
C_{D_o}	Base drag coefficient ($\alpha = 0$)
C_{L_o}	Coefficient of lift
C_{D_L}	Coefficient of drag
C'_f	Dimensionless equivalent skin friction coefficient
D	Drag force
$\vec{F}$	Total externally applied force
g	Acceleration due to gravity, assumed constant and equal to 32.17 ft per sec^2
h	Altitude
$\vec{i}$	Unit vector in the direction of total velocity
I_y	Pitch moment of inertia
$\vec{j}$	Unit vector in the lift direction
l	Reaction jet moment arm length
L	Lift force
M_x	Effective moment of inertia of control flap
m	Vehicle mass
P	Pitching torque
Q	Total heat transferred foot pounds
q	Dynamic pressure pounds per square foot
R	Range measured as arc length on the earth's surface
r_e	Earth's radius
S	Surface area
T	Thrust from reaction, jet
V	Total vehicle velocity
W	Vehicle weight

TABLE I - LIST OF SYMBOLS
(Continued)

α	Angle of attack
β	Range angle
β_A	Atmospheric pressure gradient, approximately equal to $1/23{,}500\ ft^{-1}$
γ	Flight path angle measured positive upward from the local horizontal
δ	Drag flap deflection
δ_e	Control surface deflection intended to produce pitching moment
θ	Airframe pitch angle with respect to the local horizontal
ρ	Atmospheric density slugs per cubic foot
ρ_o	Nominal sea level atmospheric density, equal to 0.0027 slugs per cubic foot

h Ft	V Ft/Sec	q Lbs/Ft^2		ω_1	ω_{1-2}/ζ_{1-2} ω_2	ω_3/ζ_3	ω_4/ζ_4	ω_5/ζ_5	z_1	z_2	z_3
190,000	23,000	200	1)	.025	100	2/.79					
			2)								
			3)	.041	98	2/.79	560/.41	590/.07	5	-8.5	12
80,000	22,700	20,000	1)	3	9.4	80/.59			5		
			2)	5.2/-.09		81/.6			5		
			3)	2.97	9.05	80/.5	540/.42	591.017	5	-98	101
25,000	14,500	100,000	1)	4.3	38	170/.2			5		
			2)	8.1	18.5	172/.23			5		
			3)	4.3	29	190/-.035	510/.5	600/.05	5	-225	223
0	7,500	60,000	1)	4.2	23	130/.31			5		
			2)	7.0	36	140/.35			5		
			3)	3.7	21	145/.13	520/.44	597/.04	5	-172	173

TABLE 2

CLOSED LOOP POLE ZERO PATTERN OF RE-ENTRY FLIGHT CONTROL SYSTEM

$$\frac{a_L}{\bar{a}_L} = \frac{\left(1+\frac{s}{z_1}\right)\left(1+\frac{s}{z_2}\right)\left(1+\frac{s}{z_3}\right)}{\left(1+\frac{s}{\omega_1}\right)\left(1+\frac{s}{\omega_2}\right)\left(1+\frac{2\zeta_3 s}{\omega_3}+\frac{s^2}{\omega_3^2}\right)\left(1+\frac{2\zeta_4 s}{\omega_4}+\frac{s^2}{\omega_4^2}\right)\left(1+\frac{2\zeta_5 s}{\omega_5}+\frac{s^2}{\omega_5^2}\right)}$$

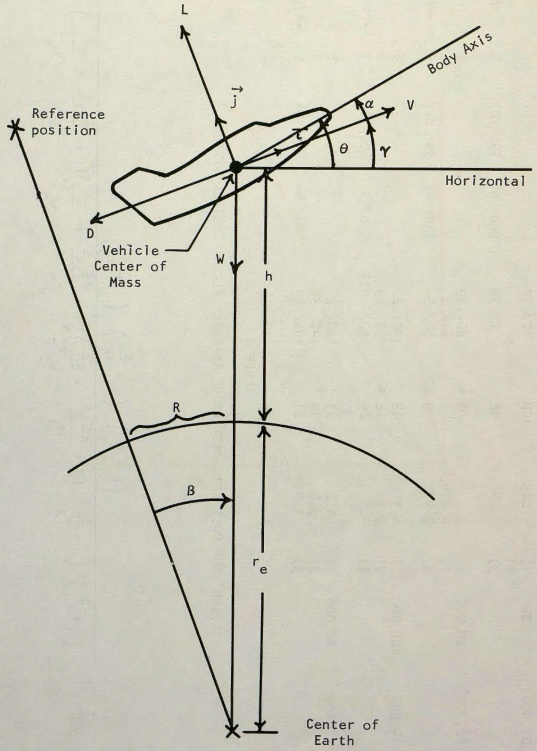

FIGURE 1 - PITCH PLANE MODEL OF A LIFTING RE-ENTRY VEHICLE

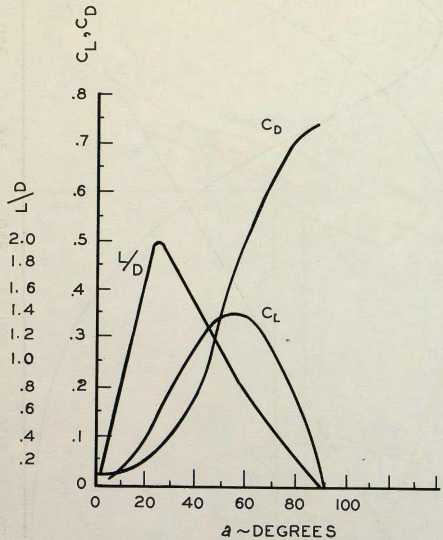

$$C_D = C_{D_0} + C_{D_L} |\sin^3 \alpha|$$

$$C_L = C_{L_0} \cos \alpha \sin \alpha |\sin \alpha|$$

$$C_{L_0} = .9$$

$$C_{D_0} = .02$$

$$C_{D_L} = .73$$

FIGURE 2 - C_L, C_D, AND L/D FOR A TYPICAL LIFTING RE-ENTRY VEHICLE

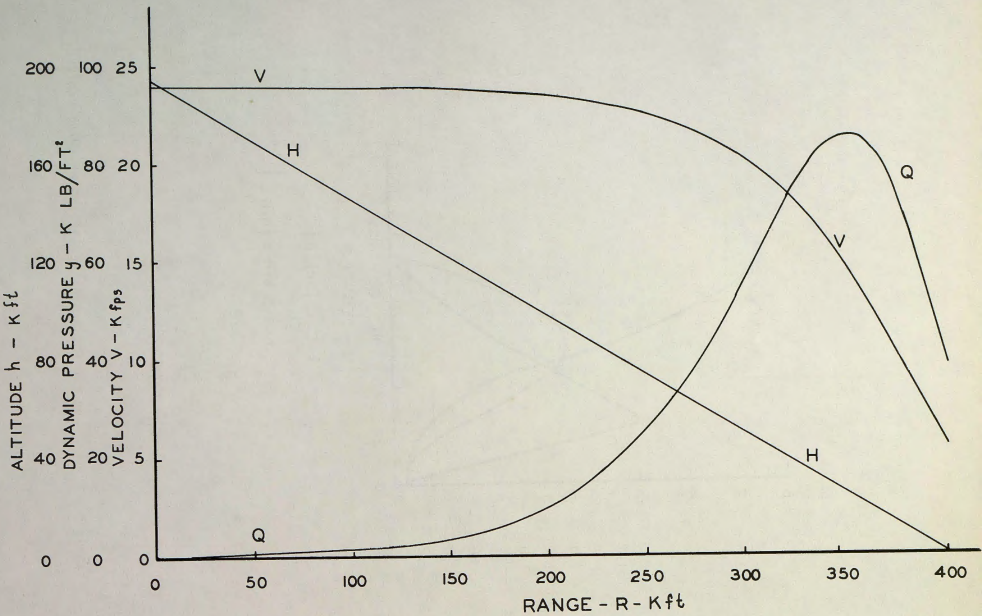

FIGURE 3 - TYPICAL BALLISTIC RE-ENTRY TRAJECTORY

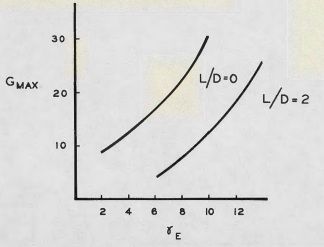

ENTRY ANGLE VS G_{MAX}

FIGURE 4 - ENTRY ANGLE VS G_{MAX}

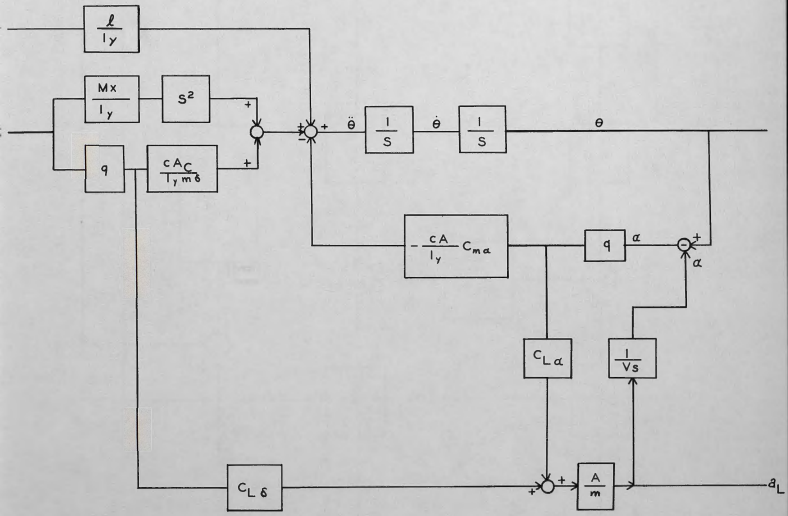

FIGURE 5 - BLOCK DIAGRAM OF LINEARIZED PITCH AXIS EQUATIONS

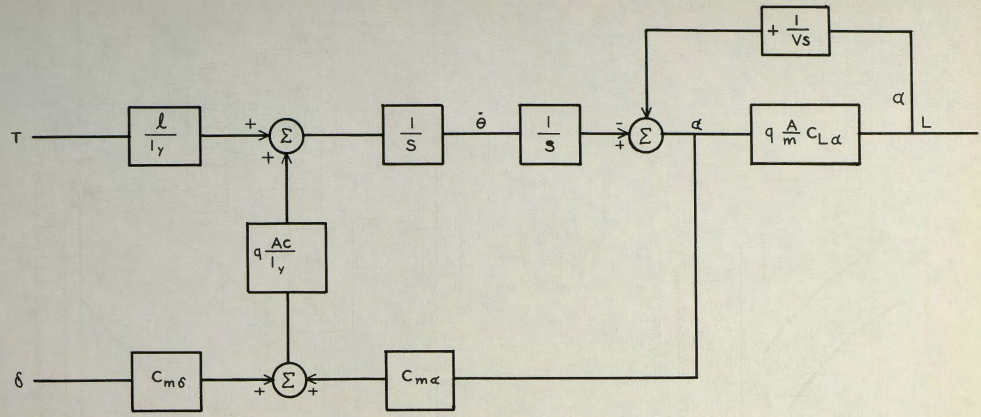

FIGURE 6 - BLOCK DIAGRAM OF LINEARIZED PITCH AXIS EQUATIONS WITH $M_x = C_{L\delta} = 0$

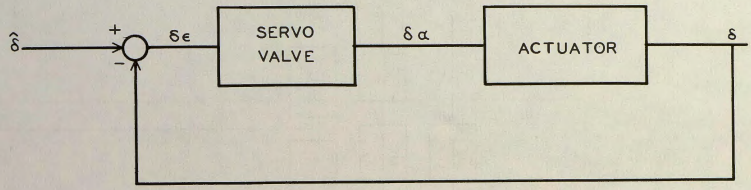

FIGURE 7 - HYDRAULIC ACTUATOR SYSTEM BLOCK DIAGRAM

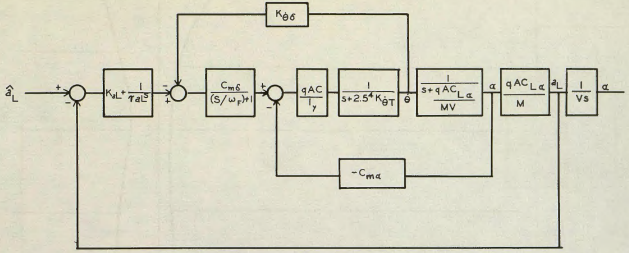

FIGURE 8 - LINEARIZED BLOCK DIAGRAM OF FLIGHT CONTROL SYSTEM

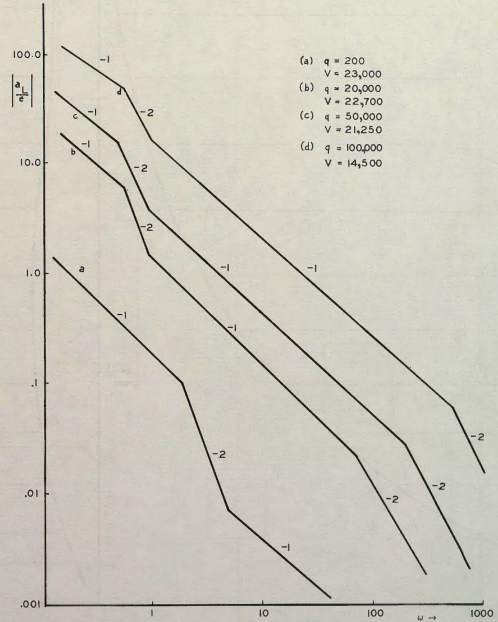

FIGURE 9 - BODE DIAGRAM OF $\left|\frac{a_L}{e}\right|$ FOR BLOCK DIAGRAM OF FIGURE 13 AND VARIOUS FLIGHT CONDITIONS

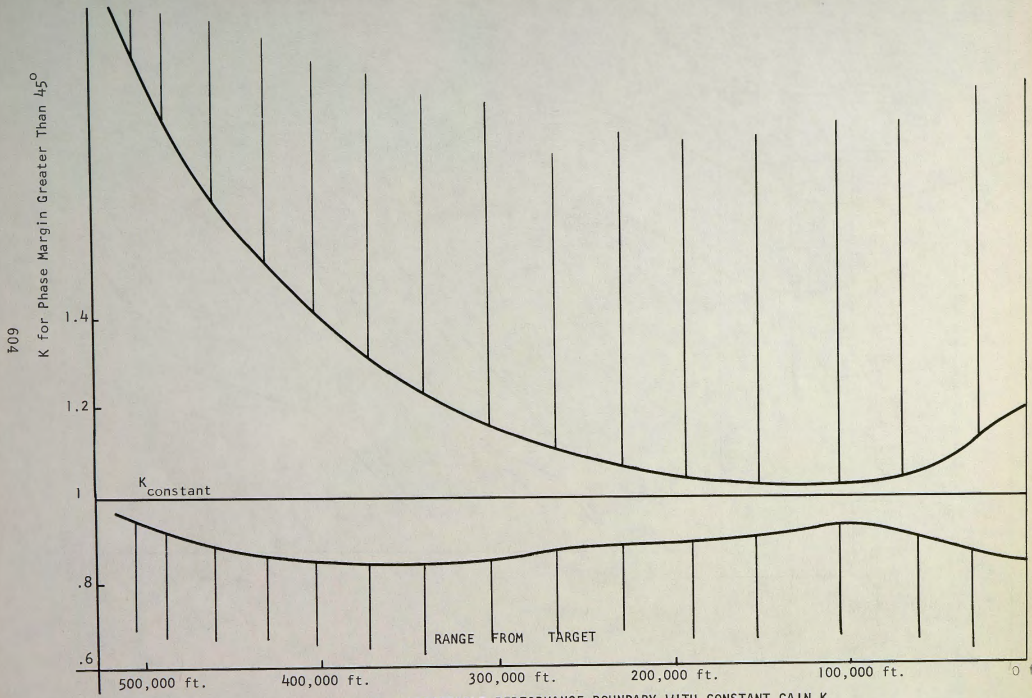

FIGURE 10 - ACCEPTABLE PERFORMANCE BOUNDARY WITH CONSTANT GAIN K

FIGURE 11 - ACCEPTABLE PERFORMANCE BOUNDARY REQUIRING ADAPTIVE CONTROL

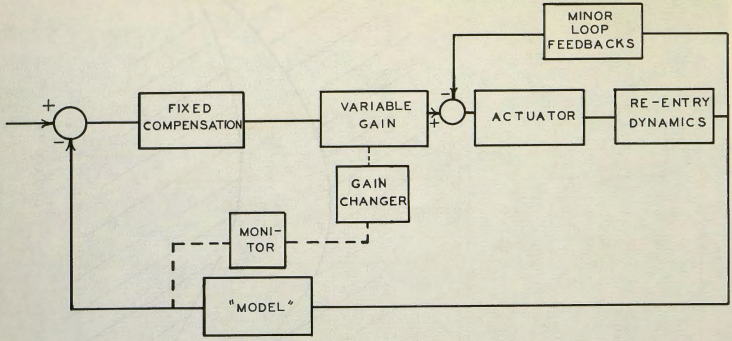

FIGURE 12 - HIGH GAIN ADAPTIVE RE-ENTRY FLIGHT CONTROL SYSTEM

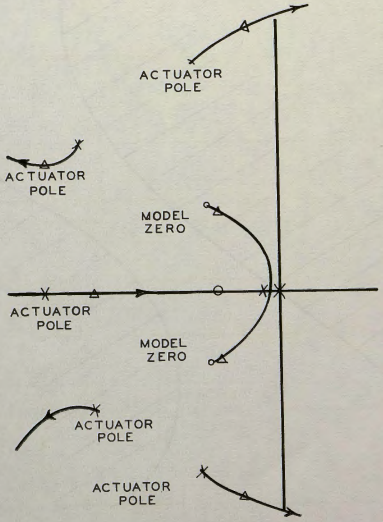

FIGURE 13 - TYPICAL ROOT LOCUS OF HIGH GAIN ADAPTIVE RE-ENTRY SYSTEM

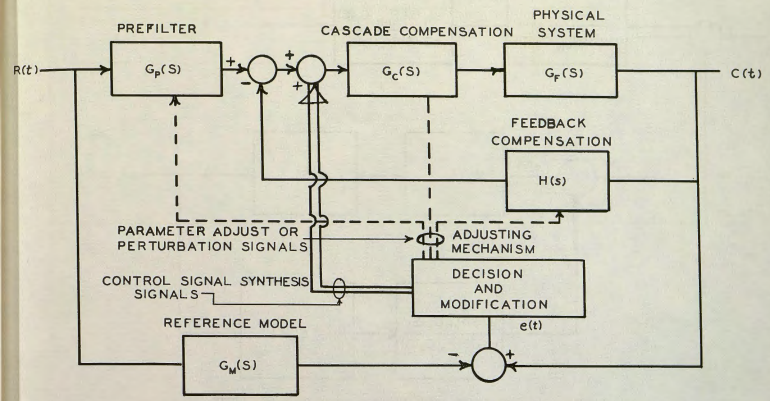

FIGURE 14 - GENERAL MODEL REFERENCE ADAPTIVE SYSTEM

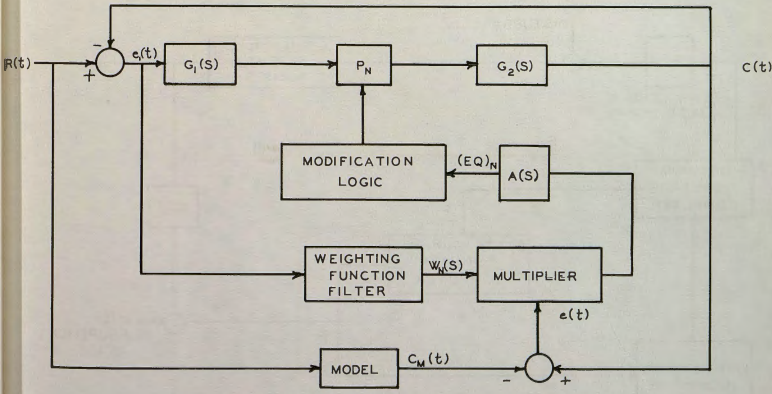

FIGURE 15 - MODEL REFERENCE PARAMETER ADJUST SYSTEM WITH ADJUSTABLE FORWARD GAIN

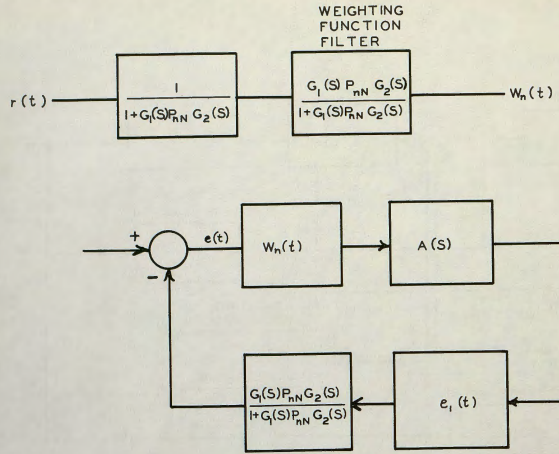

FIGURE 16 - LINEARIZED ADAPTIVE LOOP FOR SYSTEM OF FIGURE 15.

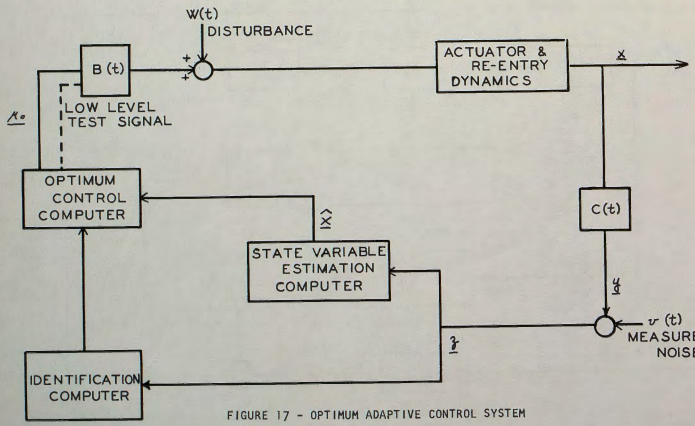

FIGURE 17 - OPTIMUM ADAPTIVE CONTROL SYSTEM

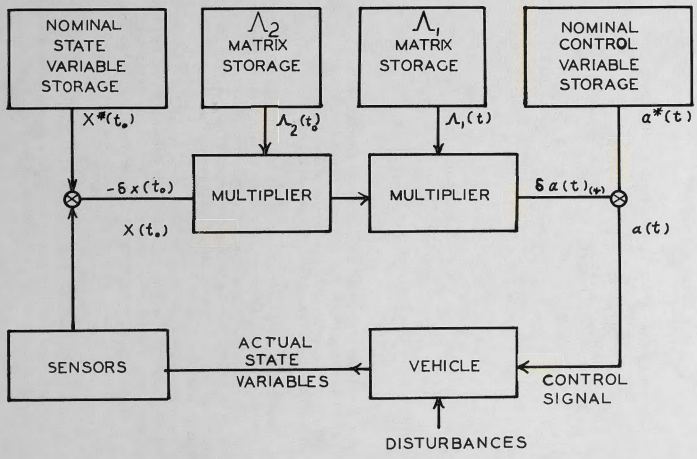

FIGURE 18 - BLOCK DIAGRAM OF Λ -MATRIX GUIDANCE SCHEME